

**EFFECT OF  $\eta$ - $\eta'$  MIXING ON  $D \rightarrow PV$  DECAYS**Bhubanjyoti Bhattacharya<sup>1</sup> and Jonathan L. Rosner<sup>2</sup>*Enrico Fermi Institute and Department of Physics**University of Chicago, 5640 S. Ellis Avenue, Chicago, IL 60637*

Charmed meson decays to a light pseudoscalar ( $P$ ) and light vector ( $V$ ) meson are analyzed taking account of  $\eta$ - $\eta'$  mixing. A frequently-used octet-singlet mixing angle of  $19.5^\circ$  is compared with a value of  $11.7^\circ$  favored by a recent analysis of  $D \rightarrow PP$  decays.

PACS numbers: 13.25.Ft, 11.30.Hv, 14.40.Lb

Decays of the charmed mesons  $D^0$ ,  $D^+$ , and  $D_s^+$  to a light pseudoscalar meson  $P$  and a light pseudoscalar meson  $V$  were analyzed within the framework of flavor SU(3) in Refs. [1] and [2]. A frequently-used octet-singlet mixing angle between  $\eta$  and  $\eta'$  of  $\theta_\eta = 19.5^\circ$  was used in Ref. [1], while Ref. [2] used  $\theta_\eta = 14.4^\circ$  based on a recent KLOE analysis [3]. In a study of  $D_{(s)} \rightarrow PP$  [4], a best fit to Cabibbo-favored decay rates was found for  $\theta_\eta = 11.7^\circ$ . In the present Brief Report we update fits to  $D_{(s)} \rightarrow PV$  decays including two decay modes not considered in [1], and compare fits based on  $\theta_\eta = 19.5^\circ$  and  $11.7^\circ$ .

We review our notation [4]. The angle  $\theta_\eta$  describing octet-singlet mixing between  $\eta$  and  $\eta'$  is defined by

$$\eta = -\eta_8 \cos \theta_\eta - \eta_1 \sin \theta_\eta, \quad \eta' = -\eta_8 \sin \theta_\eta + \eta_1 \cos \theta_\eta, \quad \text{where} \quad (1)$$

$$\eta_8 \equiv (u\bar{u} + d\bar{d} - 2s\bar{s})/\sqrt{6}, \quad \eta_1 \equiv (u\bar{u} + d\bar{d} + s\bar{s})/\sqrt{3}, \quad (2)$$

Our previous analysis of  $PV$  decays utilized  $\theta_\eta = \arcsin(1/3) = 19.5^\circ$ , for which

$$\eta = (s\bar{s} - u\bar{u} - d\bar{d})/\sqrt{3}, \quad \eta' = (2s\bar{s} + u\bar{u} + d\bar{d})/\sqrt{6}. \quad (3)$$

We consider also  $\theta_\eta = 11.7^\circ$ , for which an exact fit was found in Ref. [4] to Cabibbo-favored decays.

We refer to Ref. [1] for notation. Amplitudes defined there include color-favored tree ( $T$ ), color-suppressed tree ( $C$ ), exchange ( $E$ ), and annihilation ( $A$ ), with a subscript  $P$  or  $V$  denoting the meson containing the spectator quark. Fitting the Cabibbo-favored data quoted there, we found two solutions (“A” and “B”), distinguished by  $|T_V| < |C_P|$  (A) and  $|T_V| > |C_P|$  (B). Fits to singly-Cabibbo-suppressed data then favored solutions consistent with the set “A,” which we shall consider from now on. In Table I we show the results of this fit.

We then fit amplitudes involving  $\eta$  and  $\eta'$ , obtaining values for the amplitudes  $T_P$ ,  $C_V$ , and  $E_V$ . These are compared for the two-most-favored solutions (denoted by A1 and A2) in Tables II and III. Predictions for the branching fraction  $\mathcal{B}(D^0 \rightarrow \bar{K}^{*0} \eta')$ , listed in the last columns of Tables II and III, differ slightly between solutions A1 and A2.

Table I: Solution in Cabibbo-favored charmed meson decays to  $PV$  final states favored by fits [1] to singly-Cabibbo-favored decays.

$PV$ amplitude	Magnitude ( $10^{-6}$ )	Relative strong phase
$T_V$	$3.95 \pm 0.07$	—
$C_P$	$4.88 \pm 0.15$	$\delta_{C_P T_V} = (-162 \pm 1)^\circ$
$E_P$	$2.94 \pm 0.09$	$\delta_{E_P T_V} = (-93 \pm 3)^\circ$

Table II: Solutions for  $T_P$ ,  $C_V$ , and  $E_V$  amplitudes in Cabibbo-favored charmed meson decays to  $PV$  final states. Solutions A1 and A2 correspond to  $|T_V| < |C_P|$ . Here the  $\eta - \eta'$  mixing angle is  $\theta_\eta = 19.5^\circ$ .

No.	$PV$ ampl.	Magnitude ( $10^{-6}$ )	Relative strong phase	$\mathcal{B}(D^0 \rightarrow \bar{K}^{*0} \eta')$ ( $10^{-4}$ )
A1	$T_P$	$7.46 \pm 0.21$	Assumed 0	
	$C_V$	$3.46 \pm 0.18$	$\delta_{C_V T_V} = (172 \pm 3)^\circ$	$1.52 \pm 0.22$
	$E_V$	$2.37 \pm 0.19$	$\delta_{E_V T_V} = (-110 \pm 4)^\circ$	
A2	$T_P$	$6.51 \pm 0.23$	Assumed 0	
	$C_V$	$2.47 \pm 0.22$	$\delta_{C_V T_P} = (-174 \pm 4)^\circ$	$1.96 \pm 0.23$
	$E_V$	$3.39 \pm 0.16$	$\delta_{E_V T_V} = (-96 \pm 3)^\circ$	

Here we use a line of thought different from the analysis of Ref. [1]. We now calculate global  $\chi^2$  values for fits to singly-Cabibbo-suppressed  $D^0 \rightarrow PV$  decays for the solutions A1 and A2. We compare the  $\chi^2$  values for the fit with  $\theta_\eta = 19.5^\circ$  [including branching fractions  $\mathcal{B}(D^0 \rightarrow \eta\omega) = (0.221 \pm 0.023)\%$  [6] and  $\mathcal{B}(D^0 \rightarrow \eta\phi) = (1.4 \pm 0.5) \times 10^{-4}$  [5] omitted in the original article] with values for a fit to the same data with  $\theta_\eta = 11.7^\circ$ . These results are shown in Tables IV and V, respectively.

We see that solution A1 is favored for both  $\theta_\eta = 19.5^\circ$  and  $\theta_\eta = 11.7^\circ$ . The solution A2 is disfavored since its prediction for  $\mathcal{B}(D^0 \rightarrow \eta\phi)$  is much higher than the experimental value in both cases. The same conclusion is reached in Ref. [2] for  $\theta_\eta = 14.4^\circ$ . We will now disregard the A2 solution and only use the A1 solution for the rest of the analysis.

The next step is to use observed Cabibbo-favored decays to obtain the annihilation amplitudes  $A_P$  and  $A_V$  using the amplitudes for  $D_s \rightarrow (\bar{K}^{*0}K^+, \bar{K}^0 K^{*+}, \pi^+\omega)$  (as quoted in Table VI) and the A1 solutions. Since we use only 3 independent inputs to obtain 4 independent parameters (real and imaginary parts of  $A_P$  and  $A_V$ ) instead of obtaining unique solutions, we obtain a zone of allowed parameter space. We first form a grid of  $|A_P|$  and  $|A_V|$  values, and for every point on this grid, use the amplitudes for  $D_s \rightarrow (\bar{K}^{*0}K^+, \bar{K}^0 K^{*+})$  to obtain the phases of  $A_P$  and  $A_V$  relative to  $T_V$  (assumed real, as previously.) Thus for every point on this grid we now have an amplitude for the decay

<sup>1</sup>bhujyo@uchicago.edu

<sup>2</sup>rosner@hep.uchicago.edu

Table III: Same as Table II but with  $\theta_\eta = 11.7^\circ$ .

No.	$PV$ ampl.	Magnitude ( $10^{-6}$ )	Relative strong phase	$\mathcal{B}(D^0 \rightarrow \overline{K}^{*0} \eta')$ ( $10^{-4}$ )
A1	$T_P$	$7.69 \pm 0.21$	Assumed 0	
	$C_V$	$4.05 \pm 0.17$	$\delta_{C_V T_V} = (162 \pm 4)^\circ$	$1.19 \pm 0.12$
	$E_V$	$1.11 \pm 0.22$	$\delta_{E_V T_V} = (-130 \pm 10)^\circ$	
A2	$T_P$	$5.68 \pm 0.23$	Assumed 0	
	$C_V$	$1.74 \pm 0.23$	$\delta_{C_V T_P} = (-162 \pm 6)^\circ$	$2.19 \pm 0.16$
	$E_V$	$3.82 \pm 0.15$	$\delta_{C_V T_V} = (-87 \pm 3)^c$	

Table IV: Global  $\chi^2$  values for fits to singly-Cabibbo-suppressed  $D^0 \rightarrow PV$  decays. Also included are the process that contribute the most to a high  $\chi^2$  value. Here we have taken  $\theta_\eta = 19.5^\circ$ .

No.	Global $\chi^2$	Worst Processes (Highest $\Delta\chi^2$ values)			
		Decay Channel	$\mathcal{B}_{th}(\%)$	$\mathcal{B}_{expt}(\%)$	$\Delta\chi^2$
A1	55.9	$D^0 \rightarrow \eta \phi$	$(4.0 \pm 0.4) \times 10^{-2}$	$(1.4 \pm 0.5) \times 10^{-2}$	16.8
		$D^0 \rightarrow \eta \omega$	$0.33 \pm 0.02$	$0.221 \pm 0.023$	11.3
A2	82.4	$D^0 \rightarrow \eta \phi$	$(5.9 \pm 0.4) \times 10^{-2}$	$(1.4 \pm 0.5) \times 10^{-2}$	45.8
		$D^0 \rightarrow \pi^0 \rho^0$	$0.27 \pm 0.02$	$0.373 \pm 0.022$	10.1

$D_s \rightarrow \pi^+ \omega$  using the amplitude representation from Table VI. We now select only those points on this grid that are allowed by the experimental value  $|\mathcal{A}(D_s \rightarrow \pi^+ \omega)|$  including its one-sigma error bar.

Since there is a two-fold discrete ambiguity in choosing the phase of  $A_P$  relative to  $C_V$  or that of  $A_V$  relative to  $C_P$ , we obtain four different sets of allowed zones on the parameter space defined by  $|A_P|$  and  $|A_V|$ . The allowed zones for  $\theta_\eta = 19.5^\circ$  and  $\theta_\eta = 11.7^\circ$  are shown in Fig. 1 and Fig. 2 respectively. One may associate unique phases with  $A_P$  and  $A_V$  (that may be determined following the method explained above) for every point on the  $|A_P| - |A_V|$  plane in each of these figures.

Table V: Same as Table IV but with  $\theta_\eta = 11.7^\circ$ .

No.	Global $\chi^2$	Worst Processes (Highest $\Delta\chi^2$ values)			
		Decay Channel	$\mathcal{B}_{th}(\%)$	$\mathcal{B}_{expt}(\%)$	$\Delta\chi^2$
A1	35.8	$D^0 \rightarrow \pi^+ \rho^-$	$0.39 \pm 0.03$	$0.497 \pm 0.023$	8.5
		$D^0 \rightarrow \eta \omega$	$0.30 \pm 0.02$	$0.221 \pm 0.023$	6.7
A2	131.4	$D^0 \rightarrow \eta \phi$	$(9.2 \pm 0.6) \times 10^{-2}$	$(1.4 \pm 0.5) \times 10^{-2}$	100.0
		$D^0 \rightarrow \pi^0 \rho^0$	$0.27 \pm 0.02$	$0.373 \pm 0.022$	11.4

Table VI: Branching ratios [5] and invariant amplitudes for Cabibbo-favored decays of  $D_s$  used to obtain  $A_P$  and  $A_V$ .  $\theta_\eta$  is the  $\eta - \eta'$  mixing angle.  $\phi_1 = \arcsin(1/\sqrt{3}) = 35.3^\circ$ .

Meson	Decay mode	Representation	$\mathcal{B}$ [5] (%)	$p^*$ (MeV)	$ \mathcal{A} $ ( $10^{-6}$ )
$D_s^+$	$\overline{K}^{*0} K^+$	$C_P + A_V$	$3.9 \pm 0.6$	682.4	$3.97 \pm 0.31$
	$\overline{K}^0 K^{*+}$	$C_V + A_P$	$5.3 \pm 1.2$	683.2	$4.61 \pm 0.52$
	$\pi^+ \omega$	$\frac{1}{\sqrt{2}}(A_V + A_P)$	$0.25 \pm 0.09$	821.8	$0.76 \pm 0.14$
	$\rho^+ \eta$	$T_P \cos(\theta_\eta + \phi_1) - \frac{A_P + A_V}{\sqrt{2}} \sin(\theta_\eta + \phi_1)$	$13.0 \pm 2.2$	723.8	$6.63 \pm 0.56$
	$\rho^+ \eta'$	$T_P \sin(\theta_\eta + \phi_1) + \frac{A_P + A_V}{\sqrt{2}} \cos(\theta_\eta + \phi_1)$	$12.2 \pm 2.0$	464.8	$12.5 \pm 1.0$

Table VII: Range of predicted branching ratios for  $D_s \rightarrow (\eta, \eta') \rho^+$  using both  $\theta_\eta = 19.5^\circ$  and  $\theta_\eta = 11.7^\circ$ .

Decay mode	$\theta_\eta = 19.5^\circ$		$\theta_\eta = 11.7^\circ$	
	Min(%)	Max(%)	Min(%)	Max(%)
$\mathcal{B}(D_s \rightarrow \eta \rho^+)$	3.80	6.39	6.27	8.35
$\mathcal{B}(D_s \rightarrow \eta' \rho^+)$	2.71	3.41	2.45	3.04

To conclude one may now use the range of possible  $A_P$  and  $A_V$  values to predict  $\mathcal{B}(D_s \rightarrow \eta \rho^+)$  and  $\mathcal{B}(D_s \rightarrow \eta' \rho^+)$ . In Ref. [1] we used the solution:

$$|A_P| = 1.36_{-1.04}^{+1.16}, \quad \delta_{A_P} = (-151_{-74}^{+83})^\circ \quad (4)$$

$$|A_V| = 1.25_{-0.31}^{+0.34}, \quad \delta_{A_V} = (-19_{-9}^{+10})^\circ \quad (5)$$

which led us to obtain  $\mathcal{B}(D_s \rightarrow \eta \rho^+) = (5.6 \pm 1.2)\%$  and  $\mathcal{B}(D_s \rightarrow \eta' \rho^+) = (2.9 \pm 1.2)\%$ . Over the region of allowed values for  $A_{P(V)}$ , the central values for these Cabibbo-favored  $D_s$  branching ratios vary over the ranges shown in Table VII.

The predictions for  $\mathcal{B}(D_s \rightarrow \eta \rho^+)$  are a bit higher in the new fit using  $\theta_\eta = 11.7^\circ$  and slightly closer to the experimental value [5] quoted in Table VI. No improvement is seen in the prediction for  $\mathcal{B}(D_s \rightarrow \eta' \rho^+)$  in the new fit using  $\theta_\eta = 11.7^\circ$ . The experimental values for both these branching ratios [5], as quoted in Table VI, are much higher than the predictions using this analysis. As mentioned in Ref. [1], the relation

$$|A(D_s \rightarrow \rho^+ \eta')|^2 = |T_P|^2 + |A(D_s \rightarrow \pi^+ \omega)|^2 - |A(D_s \rightarrow \rho^+ \eta)|^2 \quad (6)$$

is very badly obeyed with the present values of  $\mathcal{B}(D_s \rightarrow \eta \rho^+)$  and  $\mathcal{B}(D_s \rightarrow \eta' \rho^+)$ , leading us to suspect either that they have been overestimated experimentally, or that disconnected diagrams (as studied in [4]) play a larger role than anticipated. The scarcity of available data for Cabibbo-favored processes prevents such an analysis in the  $D \rightarrow PV$  case.

This work was supported in part by the United States Department of Energy under Grant No. DE-FG02-90ER40560.

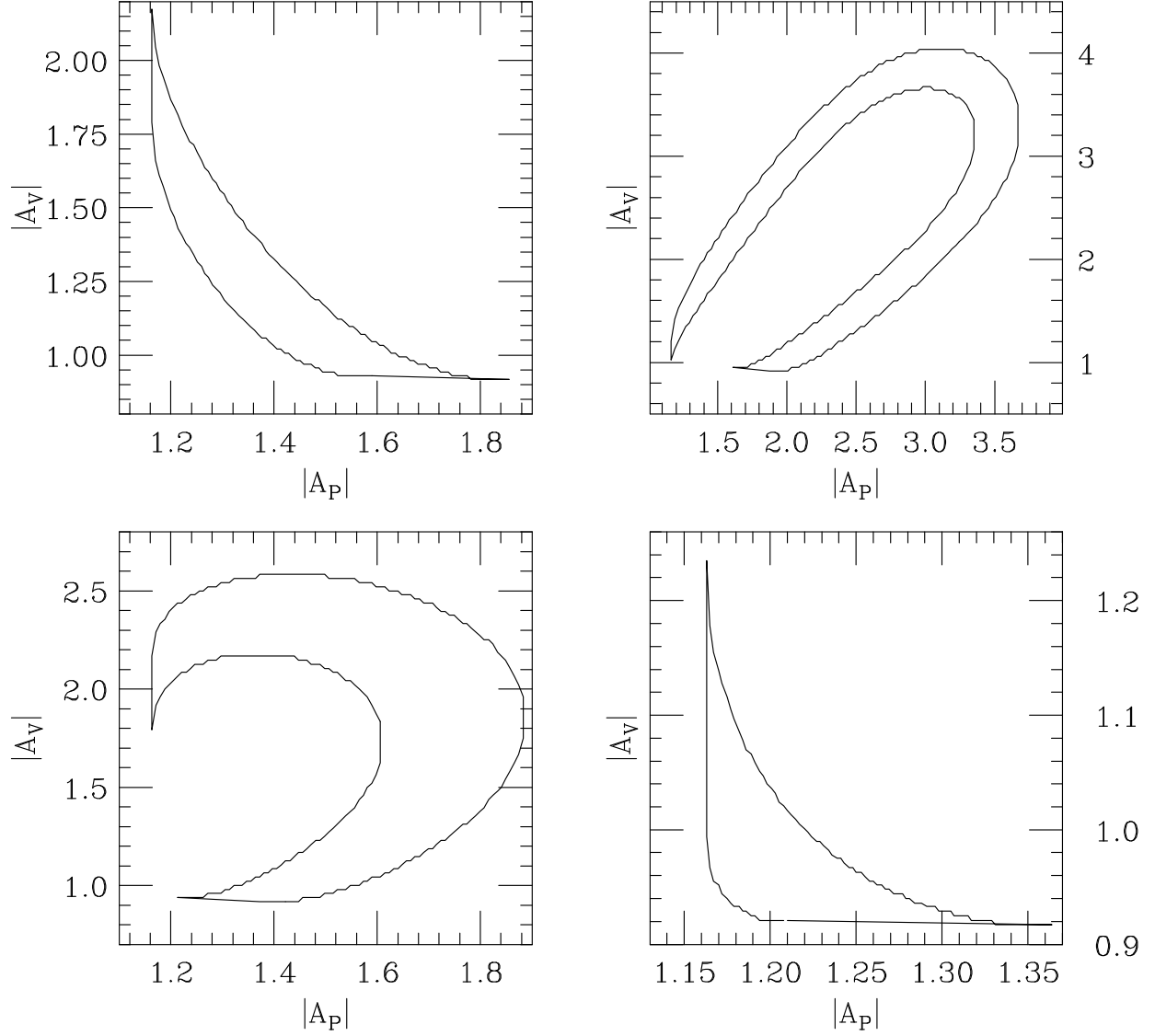


Figure 1: Allowed values for  $|A_P|$  and  $|A_V|$  for  $\theta_\eta = 19.5^\circ$ . In order to obtain the phase of  $A_{P(V)}$  we either add (denoted by  $+$ ) or subtract (denoted by  $-$ ) its phase relative to  $C_{V(P)}$  from the phase of  $C_{V(P)}$ . Clockwise from top left the 4 panels represent the phase choices: a)  $++$ , b)  $+-$ , c)  $--$  and d)  $-+$ . Thus one may associate a unique value of the phase of  $A_{P(V)}$  with every point on the parameter space in these plots.

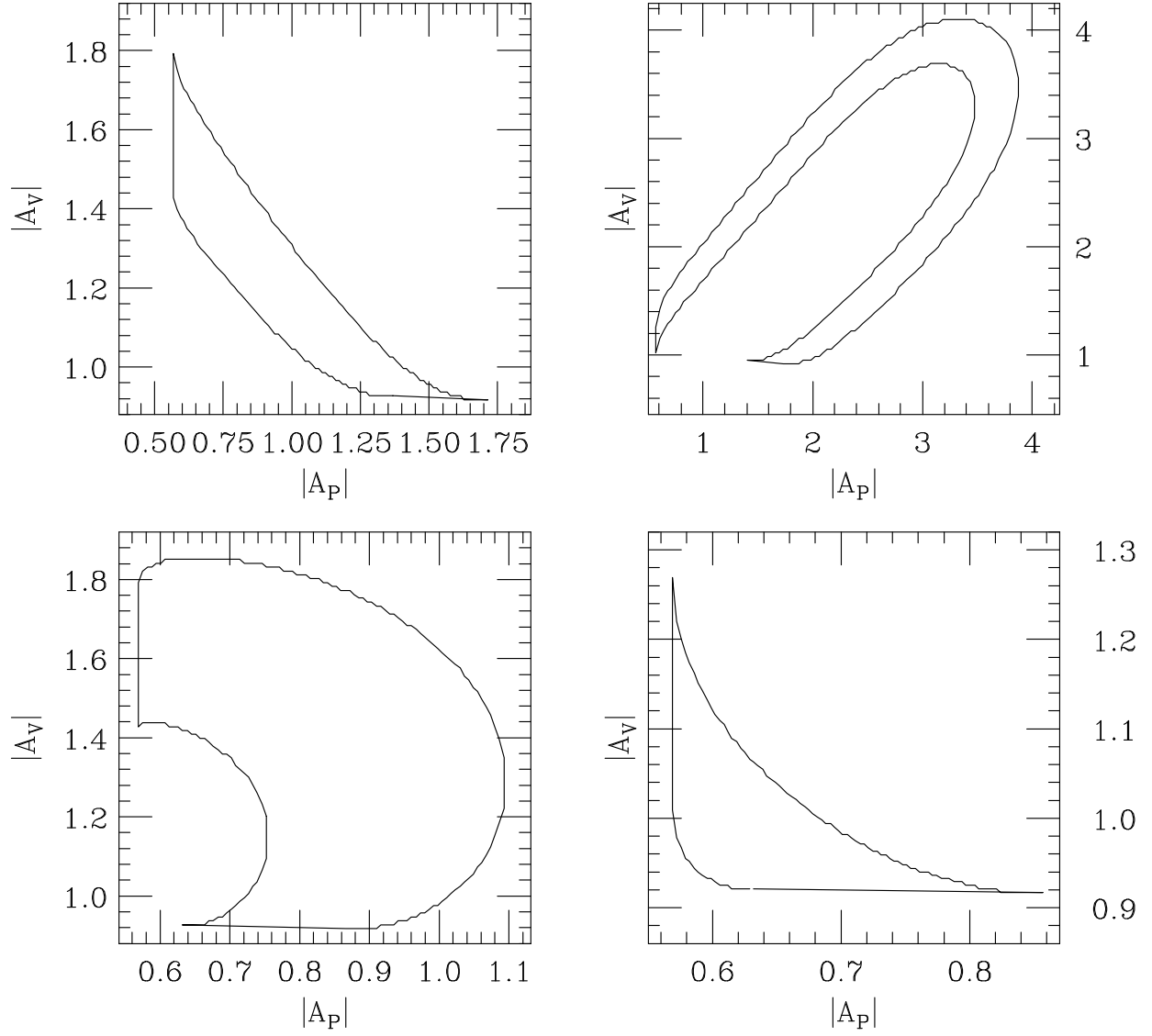


Figure 2: Same as Fig. 1 but with  $\theta_\eta = 11.7^\circ$ .

## References

- [1] B. Bhattacharya and J. L. Rosner, Phys. Rev. D **79**, 034016 (2009); Erratum, 2010, to be published.
- [2] H.-Y. Cheng and C.-W. Chiang, Phys. Rev. D **81**, 074021 (2010).
- [3] F. Ambrosino *et al.* [KLOE Collaboration], J. High Energy Phys. 07 (2009) 105.
- [4] B. Bhattacharya and J. L. Rosner, Phys. Rev. D **81**, 014026 (2010).
- [5] C. Amsler *et al.* (Particle Data Group), Phys. Lett. B **667**, 1 (2008), and partial 2009 update for the 2010 edition of Review of Particle Physics.
- [6] R. Kass [BaBar Collaboration], presented at EPS2009, Krakow, Poland, <http://pos.sissa.it/cgi-bin/reader/conf.cgi?confid=84>.